Vibrational spectra of light and heavy water with application to neutron cross section calculations

J. I. Marquez Damian, D. C. Malaspina, and J. R. Granada

Citation: J. Chem. Phys. **139**, 024504 (2013); doi: 10.1063/1.4812828
View online: http://dx.doi.org/10.1063/1.4812828
View Table of Contents: http://jcp.aip.org/resource/1/JCPSA6/v139/i2
Published by the AIP Publishing LLC.

Vibrational spectra of light and heavy water with application to neutron cross section calculations

J. I. Marquez Damian,[1,a)] D. C. Malaspina,[2] and J. R. Granada[1,b)]
[1]*Neutron Physics Department and Instituto Balseiro, Centro Atómico Bariloche, CNEA, Argentina*
[2]*Department of Biomedical Engineering and Chemistry of Life Processes Institute, Northwestern University, 2145 Sheridan Road, Evanston, Illinois 60208, USA*

(Received 4 June 2013; accepted 19 June 2013; published online 11 July 2013)

The design of nuclear reactors and neutron moderators require a good representation of the interaction of low energy ($E < 1$ eV) neutrons with hydrogen and deuterium containing materials. These models are based on the dynamics of the material, represented by its vibrational spectrum. In this paper, we show calculations of the frequency spectrum for light and heavy water at room temperature using two flexible point charge potentials: SPC-MPG and TIP4P/2005f. The results are compared with experimental measurements, with emphasis on inelastic neutron scattering data. Finally, the resulting spectra are applied to calculation of neutron scattering cross sections for these materials, which were found to be a significant improvement over library data. © *2013 AIP Publishing LLC*. [http://dx.doi.org/10.1063/1.4812828]

I. INTRODUCTION

In nuclear reactors and other nuclear systems, light and heavy water and other hydrogen and deuterium containing materials are used as moderators to reduce the energy of neutrons through collisions in the material. At neutron energies well above the characteristic excitations of a condensed matter system ($\geq$1 eV), the free-gas approximation is appropriate to describe the interaction with the scattering units, and data thus calculated are borne into the cross section libraries. However, at lower neutron energies, the actual structure and dynamics of the scattering system must be accounted for to attain a realistic description of thermal neutron scattering processes. Despite the advances in neutron measurements and modeling, these calculations use thermal neutron interaction data (represented as a scattering function or scattering law, $S(\kappa, \omega)$) extracted from evaluated nuclear data libraries[1] that are still produced with models that use frequency spectra based on experimental data from the 1960s.[2,3]

Molecular dynamics (MD) methods offer a powerful tool to obtain microscopic information of the molecular motions of liquid water and provide a background for the interpretation of experimental data: calculations of the frequency spectra of water from MD using flexible models show good agreement with experiments.[4–9] In particular, Martí, Padro, and Guàrdia[8] did an extensive work to calculate the frequency spectra of liquid light and heavy water at different temperatures and pressures using a flexible SPC water model (SPC-MPG). More recently, Lisichkin[9] compared these results with experimental data from inelastic neutron scattering in light water.[10]

In this paper, we extend the work by Marti *et al.*,[8] and by Lisichkin *et al.*,[9] comparing vibrational spectra calculations using SPC-MPG and TIP4P/2005f flexible potentials for both light and heavy water. These results are then compared with experimental (infrared spectroscopy and inelastic neutron scattering) data and used to create models to compute the scattering law and neutron scattering cross sections.

II. MOLECULAR DYNAMICS SIMULATIONS

The MD simulations were performed using the GROMACS simulation package, v.4.5.5.[11] The simulated systems consist of 512 water molecules in a cubic box with periodic boundary conditions. The dynamic equations were integrated using the leapfrog algorithm with a time-step of 0.1 fs in a isobaric-isothermal ensemble with a production run of 100 ps. The temperature was $T = 300$ K, controlled using the Nosé-Hoover thermostat with a time constant of 0.1 ps and the pressure was $P = 1$ bar maintained by a Parrinello-Rahman barostat with a time constant of 0.5 ps and compressibility of 4.5 $\times 10^{-5}$ bar^{-1}. A spherical cutoff of 0.9 nm was imposed for the Lennard-Jones and the electrostatic contributions with no long-range electrostatic for the SPC-MPG model and using particle mesh Ewald algorithm for the TIP4P/2005f model.

The water models implemented for the calculation are the SPCE flexible model[4] parametrized by Marti, Padro, and Guardia[12] (SPC-MPG) and the TIP4P/2005 flexible model, parametrized by Gonzalez and Abascal[13] (TIP4P/2005f).

The functional form of the potential for SPC-MPG model is

$$V = \sum_{i \neq j} 4\epsilon_{\mathrm{O}} \left[\left(\frac{\sigma_{\mathrm{O}}}{r_{\mathrm{O}_i\mathrm{O}_j}} \right)^{12} - \left(\frac{\sigma_{\mathrm{O}}}{r_{\mathrm{O}_i\mathrm{O}_j}} \right)^{6} \right] + f \frac{q_i q_j}{r_{ij}}$$
$$+ D_{\mathrm{OH}}[1 - \mathrm{e}^{-\beta_{\mathrm{OH}}(r_{\mathrm{OH}} - b\mathrm{OH})}]^2 + \frac{1}{2} k_{\mathrm{H_1H_2}} (r_{\mathrm{H_1H_2}} - b_{\mathrm{H_1H_2}})^2$$
$$+ k_{rr}(|r_{\mathrm{O}} - r_{\mathrm{H_1}}| - r_{rr1})(|r_{\mathrm{O}} - r_{\mathrm{H_2}}| - r_{rr2})$$
$$+ k_{r\theta}(|r_{\mathrm{H_1}} - r_{\mathrm{H_2}}| - r_{r\theta 1})$$
$$\times (|r_{\mathrm{O}} - r_{\mathrm{H_1}}| - r_{r\theta 2} + |r_{\mathrm{O}} - r_{\mathrm{H_2}}| - r_{r\theta 3}). \quad (1)$$

a)Author to which correspondence should be addressed. Electronic mail: marquezj@cab.cnea.gov.ar.
b)Also at Consejo Nacional de Investigaciones Cientificas(CONICET), Argentina.

TABLE I. Parameters for SPC-MPG and TIP4P/2005f models.

Parameter	SPC-MPG	TIP4P/2005f
ϵ_O(kJ mol^{-1})	0.65014	0.77490
σ_O(nm)	0.31656	0.31644
q_O(e)	− 0.82	0.0
q_H(e)	0.41	0.5564
q_M(e)	...	− 1.1128
d_{OM}(nm)	...	0.1555
d_{OH}(nm)	0.1000	0.09664
d_{HH}(nm)	0.1633	...
θ_0(deg)	...	104.79
D(kJmol^{-1})	401.67	432.581
β(nm^{-1})	25.67	22.87
k_{HH}(kJ mol^{-1} nm^{-2})	102193.34	...
k_{rr}(kJ mol^{-1} nm^{-2})	52993.6	...
$k_{r\theta}$(kJ mol^{-1} nm^{-2})	− 77081.6	...
k_θ(kJ mol^{-1} rad^{-2})	...	367

And the functional form for the TIP4P/2005f is

$$V = \sum_{i\neq j} 4\epsilon_O \left[\left(\frac{\sigma_O}{r_{O_iO_j}}\right)^{12} - \left(\frac{\sigma_O}{r_{O_iO_j}}\right)^{6}\right] + \sum_{i\neq j} f\frac{q_i q_j}{r_{ij}} + D[1 - e^{-\beta(r_{OH_i} - d_{OH})}]^2 + \tfrac{1}{2}k_\theta\,(\theta_{HOH} - \theta_0)^2\,, \quad (2)$$

where O, H_1, H_2 subscripts indicate the oxygen and hydrogen sites, respectively, and i, j two different water molecules.

Both models have a repulsive Lennard-Jones potential on the oxygen and the charges are distributed in the oxygen and hydrogen sites. The stretching O–H potential is modeled in both cases with an anharmonic Morse potential. H–O–H bending, in the case of SPC-MPG, is modeled with three potentials: an harmonic H–H bond, a cross bond-bond potential for the H–O–H, and a cross angle potential for the H–O–H also. In TIP4P/2005f, the H–O–H bending is modeled with an harmonic angle potential. The parameters for the two models are listed in Table I.

For heavy water we implemented the same water potentials but modifying the mass of the H. In general this is an acceptable approximation as we can observe from the results below.

III. CALCULATION OF FREQUENCY SPECTRA

The vector with velocities was stored in the trajectory file every 0.6 fs and then processed with the GROMACS tool `g_velacc` to compute the velocity autocorrelation function

$$\mathrm{VACF}_\alpha(\tau) = \langle v_\alpha(t)\cdot v_\alpha(t+\tau)\rangle\,,$$

where $\langle\cdot\rangle$ is the ensemble average over a particular group of atoms (D, H, O).

TABLE II. Self-diffusion coefficients for light and heavy water at 300 K ($D/10^{-9}$m^2 s^{-1}).

	H_2O	D_2O
SPC-MPG	2.75	2.44
TIP4P/2005f	2.20	1.82
Mills (Exp.)	2.35	1.96

Using these results, frequency spectra can be computed as the Fourier transform of the VACF,

$$\rho(\omega) = \frac{\frac{1}{2\pi}\int_{-\infty}^{\infty}\langle v\cdot v(t+\tau)\rangle\, e^{-i\omega\tau}d\tau}{\int_0^\infty \frac{1}{2\pi}\int_{-\infty}^{\infty}\langle v\cdot v(t+\tau)\rangle\, e^{-i\omega\tau}d\tau d\omega} = \frac{\frac{1}{2\pi}\int_{-\infty}^{\infty}\langle v\cdot v(t+\tau)\rangle\, e^{-i\omega\tau}d\tau}{\frac{1}{2}\langle v(\tau)^2\rangle e^{-i\omega\tau}d\tau d\omega} = \frac{M}{3\pi kT}\frac{1}{2\pi}\int_{-\infty}^{\infty}\mathrm{VACF}(\tau)e^{-i\omega\tau}d\tau,$$

where $\mathrm{VACF}(\tau) = \mathrm{VACF}(-\tau)$ for $\tau < 0$.

From this expression we computed the frequency spectra for H and O in H_2O, and for D and O in D_2O.

The resulting frequency spectra includes all the dynamical modes of the molecule and the liquid. From lower to higher energy: diffusion, intermolecular vibrations, librations, and intramolecular vibrations. In the limit $\rho(\epsilon \to 0)$, the only dynamic mode present is diffusion, and the spectrum is proportional to the diffusion coefficient

$$\lim_{\varepsilon\to 0}\rho\,(\varepsilon) = \frac{2m_i D}{\pi\hbar}. \quad (3)$$

The computed values of the diffusion coefficient for H_2O and D_2O are compared in Table II with values interpolated from measurements by Mills.[14]

The computed frequency spectra can be compared with experimental results from inelastic neutron scattering (INS) and infrared spectroscopy, although there are differences that have to be taken into account in these comparison.

In the case of infrared spectroscopy, the quantity that is usually regarded as the infrared spectrum (i.e., the infrared absorption coefficient) is not proportional to the frequency spectrum, but it is related to the absorption line shape, which can be computed from the dipolar correlation function[15] because the interaction is electromagnetic in nature. Nevertheless, the infrared absorption coefficient is a good measurement of the energy of the different dynamical modes. A comparison of predicted energies of the different intramolecular vibration modes with Fourier-transform infrared attenuated total reflection (FTIR-ATR) spectroscopy measurements[16] are shown in Figures 1 (H_2O) and 2 (D_2O).

In the case of inelastic neutron scattering, the frequency spectrum is derived from measurements in spectrometers, which measure the intensity of the scattered neutrons at different outgoing energies and angles. After applying multiple scattering corrections, to take into account the finite size of the sample, and computing the scattering function, the frequency spectrum is either extracted by doing a one-phonon

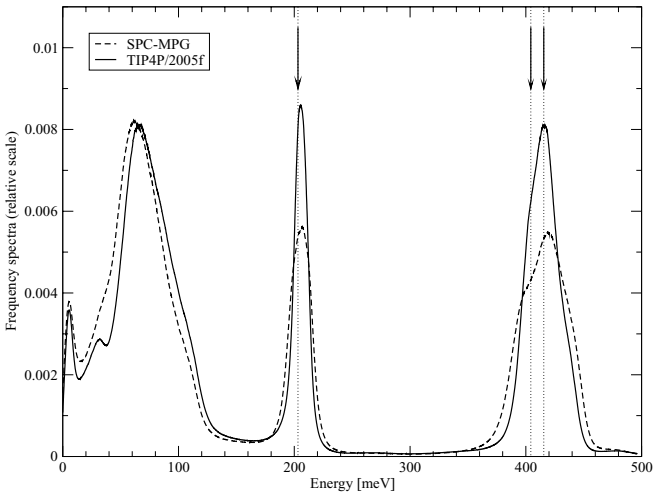

FIG. 1. Intramolecular vibrational spectra for light water. Arrows point at normal mode energies obtained by Lappi[16] using FTIR-ATR.

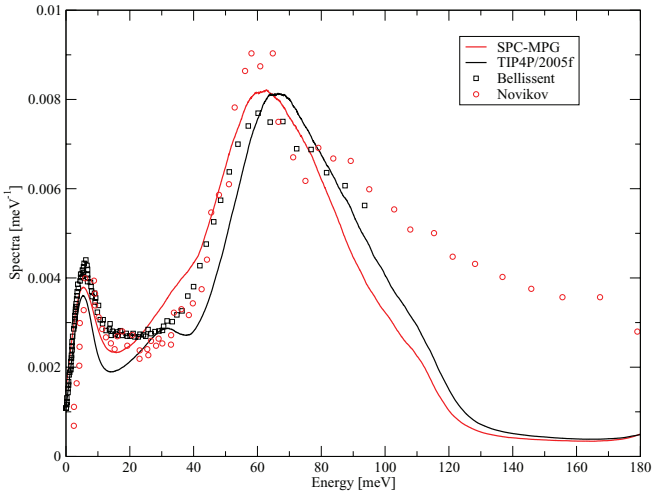

FIG. 3. Calculated low energy frequency spectrum for light water compared with measurements by inelastic neutron scattering.

approximation, or by performing an extrapolation to $Q \to 0$. Experiments designed to use the one phonon approximation usually use low incident neutron energies and have a narrow range of measurement. Experiments designed to use the Egelstaff-Schofield extrapolation technique usually cover a wider energy range, but may have artifacts caused by multiphonon scattering.

Figure 3 shows the spectrum of H_2O compared with measurements by Bellissent-Funel[17] and Novikov.[10] For this plot, the experimental values were re-normalized to approximately the same area below the peak of the librational band, to make comparable measurements that are not absolute in nature. The calculated spectrum of H_2O is computed as the weighted average of the spectra for H and O,

$$\rho_{H_2O}(\epsilon) = \frac{2\sigma_H \rho_H(\epsilon) + \sigma_O \rho_O(\epsilon)}{2\sigma_H + \sigma_O}, \quad (4)$$

where σ_H and σ_O are, respectively, the bound-atom scattering cross sections for hydrogen and oxygen.

The measurements by Novikov show a librational band that stretches up in the higher frequency region, which are not observed neither in previous experimental measurements[18] nor in other molecular dynamics calculations[9] and could be interpreted as librational overtones that survived the multiphonon correction of the spectrum. Overall, both experimental and calculated results show the same features: a peak at ~6 meV, which is usually interpreted[19] as O–O–O bending in the hydrogen bond network, and a librational band centered at ~60 meV. Leaving aside the higher end of the librational band mentioned above, the relative weight between these two modes is similar in both experimental and computed results.

For heavy water the experimental results are more sparse: only measurements by Von Blanckenhagen,[20] Larsson,[21] and Haywood[18] could be found in the literature. A comparison with computed results is shown in Fig. 4.

In the case of light water the high scattering cross section of ^{1}H ($\sigma_H = 82.02$ b) compared to ^{16}O ($\sigma_O = 4.232$ b) makes the neutron-weighted molecular frequency spectrum to be dominated by the vibrational spectrum of hydrogen. In the

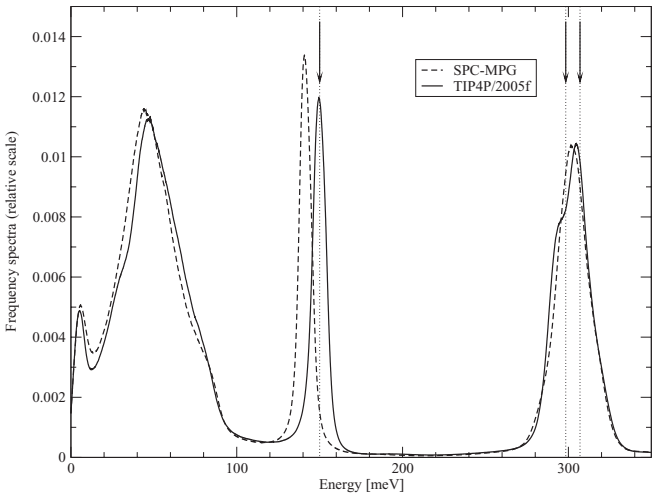

FIG. 2. Intramolecular vibrational spectra for heavy water. Arrows point at normal mode energies obtained by Lappi[16] using FTIR-ATR.

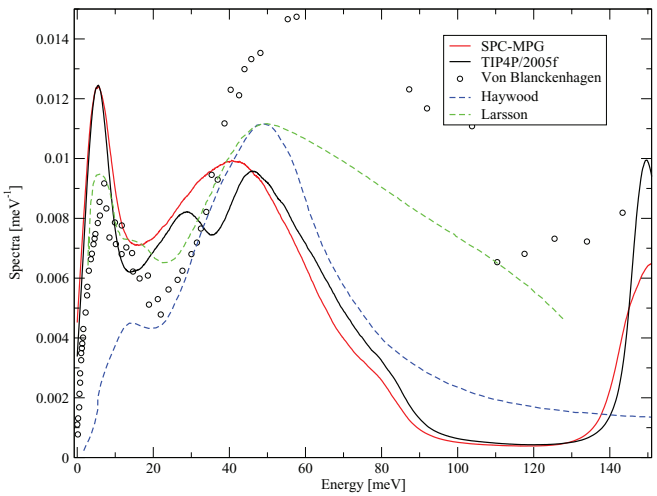

FIG. 4. Calculated low energy frequency spectrum for heavy water compared with measurements by inelastic neutron scattering.

case of heavy water, the difference is smaller ($\sigma_D = 7.64$ b) and the measurement of the frequency spectrum with neutrons show both an intense response in the librational band (by the deuterium) and in the inter-molecular vibrations (by the oxygen). The comparison with experimental data is not conclusive, and the experimental data are not in complete agreement between the different sets. Nevertheless, the intermolecular bending mode at ~5 meV is also seen in the measurements by Von Blanckenhagen[20] and by Larsson,[21] and the librational band at ~50 meV observed in the results from Haywood[18] and from Larsson[21] is slightly higher than the computed values.

IV. APPLICATIONS

Using the LEAPR[3] module of the software package NJOY,[22] we computed the scattering function for H and O in H_2O, and for D and O in D_2O. The scattering function is defined as

$$\frac{d\sigma}{dE'\Omega'} = \frac{\sigma_b}{4\pi kT} \cdot \sqrt{\frac{E'}{E}} \cdot S(\alpha, \beta),$$

where $\frac{d\sigma}{dE'\Omega'}$ is the double differential scattering cross section of neutrons with incident energy E, outgoing energy E' and direction change Ω', and α and β are the adimensionalized changes of momentum and energy

$$\alpha = \frac{1}{MkT}[E' + E - 2\sqrt{EE'}\cos\theta], \ \beta = \frac{E - E'}{kT}.$$

In LEAPR the scattering function is computed using the incoherent approximation as the convolution of a diffusion scattering function (S_{diff}), and a scattering function computed from the remaining continuous spectrum (S_{cont}),

$$S(\alpha, \beta) = S_{\text{diff}} \otimes S_{\text{cont}}. \tag{5}$$

The diffusion component is computed using the Egelstaff-Schofield diffusion model,[23] and continuous spectrum component is computed using a phonon expansion of the gaussian approximation

$$S_{\text{diff}}(\alpha, \beta) = \frac{2cw_t\alpha}{\pi} \exp\left[2c^2w_t\alpha - \beta/2\right] \times \frac{\sqrt{c^2 + 1/4}}{\sqrt{\beta^2 + 4c^2w_t^2\alpha^2}} K_1\left[\sqrt{c^2 + 1/4}\sqrt{\beta^2 + 4c^2w_t^2\alpha^2}\right], \tag{6}$$

$$S_{\text{cont}}(\alpha, \beta) = \frac{1}{2\pi}\int_{-\infty}^{\infty} d\hat{t}\ e^{i\beta\hat{t}}e^{-\gamma(\hat{t})}, \tag{7}$$

$$\gamma\left(\hat{t}\right) = \alpha\int_{-\infty}^{\infty} d\beta\ \frac{\rho(\beta)e^{\beta/2}}{2\beta\sinh\left(\beta/2\right)}[1 - e^{-i\beta\hat{t}}], \ \hat{t} = tkT/\hbar. \tag{8}$$

In the case of hydrogen, the incoherent approximation is sufficient, whereas for deuterium and oxygen a correction for coherent effects is needed. We used the Sköld correction[24]

$$S^D_{\text{coh}}(\alpha, \beta) = S^D_{\text{inc}}(\alpha/\tilde{S}^D(Q), \beta)\tilde{S}^D(Q),$$

$$\tilde{S}^D(Q) = 1 + \frac{2}{3}\left[S_{DD}(Q) - 1\right] + \frac{1}{3}\frac{b^O_{\text{coh}}}{b^D_{\text{coh}}}\left[S_{DO}(Q) - 1\right],$$

$$S^O_{\text{coh}}(\alpha, \beta) = S^O_{\text{inc}}(\alpha/\tilde{S}^O(Q), \beta)\tilde{S}^O(Q),$$

$$\tilde{S}^O(Q) = 1 + \frac{2}{3}\left[S_{OO}(Q) - 1\right] + \frac{1}{3}\frac{b^D_{\text{coh}}}{b^O_{\text{coh}}}\left[S_{DO}(Q) - 1\right],$$

where $S_{\text{ij}}(Q) = S_{\text{DO}}(Q)$, $S_{\text{DO}}(Q)$, $S_{\text{DD}}(Q)$ are the partial structure factors of heavy water, obtained by Soper.[25]

Using the calculated scattering functions, several measurable neutron scattering quantities were computed. The results were compared with experimental data and with calculations performed with scattering kernels distributed in the nuclear

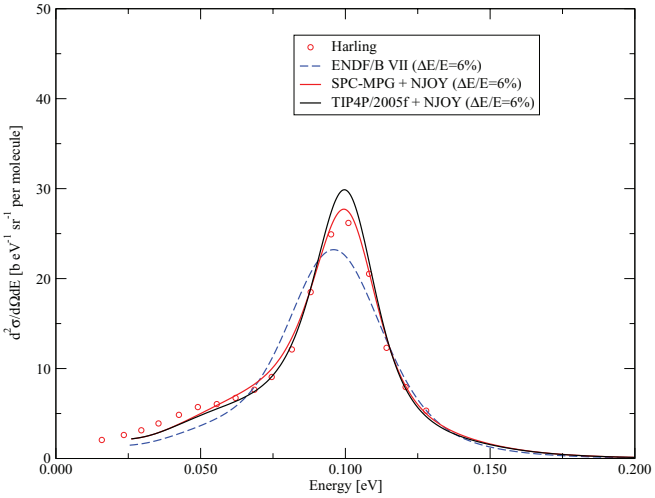

FIG. 5. Double differential scattering cross section for heavy water, $E_0 = 101$ meV, $\theta = 60°$.

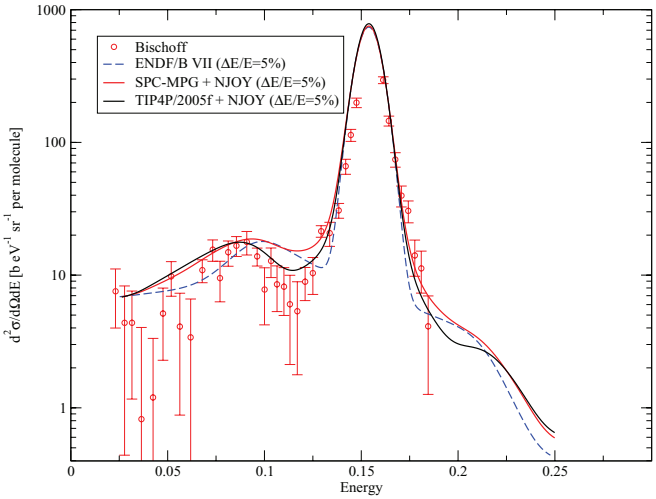

FIG. 6. Double differential scattering cross section for light water, $E_0 = 154$ meV, $\theta = 14°$.

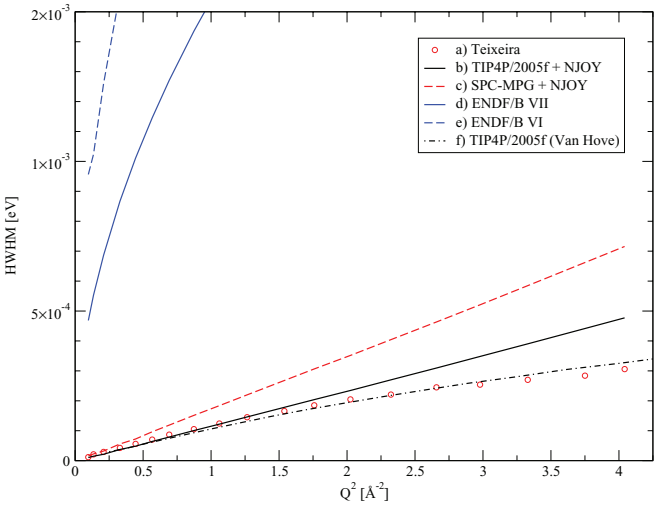

FIG. 7. Quasi-elastic scattering half-width for light water for $E_0 = 3.15$ meV measured by Teixeira[28] (curve a). Curves b and c are the quasi-elastic HWHM computed from TIP4P/2005f and SPC-MPG spectra, respectively, which coincide with DQ^2. Curves d and e are the HWHM computed from ENDF/B VII and ENDF/B VI. Curve f is the HWHM computed from the Fourier transform of $G_s(r, t)$. The calculations were performed at the experimental temperature, 293 K.

data libraries.[1] Starting from the double differential cross sections, a general good agreement was found with experimental data from Harling[26] (heavy water, Fig. 5) and Bischoff[27] (light water, Fig. 6).

A more stringent test of the low energy dynamics is given by the width of the quasi-elastic peak at low incident energies. The results for light water (Fig. 7) show a much better agreement with the data from Teixeira[28] than ENDF/B VII (Evaluated Nuclear Data File, version 7), because existing libraries were computed using a free gas approximation instead

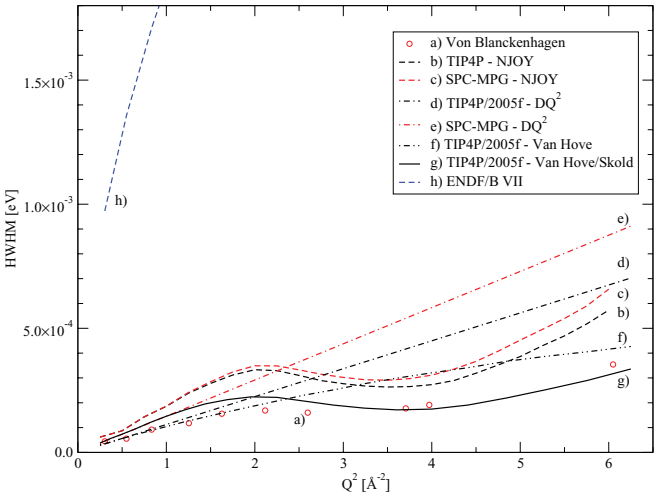

FIG. 8. Quasi-elastic scattering half-width for heavy water for $E_0 = 5$ meV measured by Von Blanckenhagen[20] (curve a). Curves b and c are the calculations computed with NJOY and the Sköld approximation, which introduces a structure correction to the diffusion results (curves d and e). Curve f is the halfwidth computed as the Fourier transform of $G_s(r, t)$, and g is the halfwidth computed as the Fourier transform of $G_s(r, t)$, including Sköld corrections. Curve h is the HWHM computed with the ENDF/B VII library. The calculations were performed at the experimental temperature, 296 K.

of diffusion. Nevertheless, the rather simple diffusion model included in NJOY cannot reproduce the jump diffusion behavior found by Teixeira[28] at high Q^2. If such correction is necessary, $S(\alpha, \beta)$ can be computed directly from the Van Hove self-correlation function by Fourier transform (curve f in Fig. 7),

$$S_i(\alpha, \beta) = \frac{kT}{2\pi} \int G_s(\vec{r}, t) e^{\vec{k}\cdot\vec{r} - \omega t} \mathrm{d}\vec{r}\, \mathrm{d}t, \tag{9}$$

where $G_s(r, t)$ can be computed from the GROMACS trajectory file.

In the case of heavy water (Fig. 8), the width of the quasi-elastic peak depends not only in the dynamics but also in the structure, which can be seen in the experimental results from Von Blanckenhagen.[20] The calculations in the Sköld approximation appear as oscillations around the DQ^2 behavior produced by the diffusion model in LEAPR. Again, if further improvement is needed for low energy transfers, $S(\alpha, \beta)$ can be calculated directly from $G_s(r, t)$ (curve g in Fig. 8) and corrected using the Sköld approximation (curve h in Fig. 8).

V. CONCLUSIONS

SPC-MPG and TIP4P/2005f models are suitable tools for the calculation of the vibrational spectra of light and heavy water. In both models, intramolecular potentials are adjusted to reproduce the internal vibrations of light and heavy water, as observed by FTIR. For the collective molecular motion, TIP4P/2005f shows a better agreement in the calculation of the diffusion coefficient, at the expense of a more marked intermolecular bending (acoustic) mode and the hardening of the librational band.

In the case of heavy water there is a considerable discrepancy between calculations and experimental values. But, considering the differences that can be observed between different experiments, we think that this calls for new measurements of the frequency spectrum of heavy water with state of the art neutron scattering instruments and data processing algorithms.

The application of these calculated frequency spectra to neutron scattering cross sections calculations show that molecular dynamics is a valuable tool for the evaluation of the scattering law in classical liquids. Although, for the calculation of low energy transfers the methodology is insufficient and it might be useful to compute the scattering law from the Van Hove autocorrelation function. Using these tools, a new evaluation of the scattering law for light and heavy water is planned to be presented.

ACKNOWLEDGMENTS

The J. I. Marquez Damian and J. R. Granada wish to acknowledge the support provided by CONICET. D. C. Malaspina acknowledges the support from National Science Foundation (NSF) (Grant No. CHE-0957653).

[1] M. B. Chadwick, M. Herman, P. Obložinský, M. E. Dunn, Y. Danon, A. C. Kahler, D. L. Smith, B. Pritychenko, G. Arbanas, R. Arcilla *et al.*, Nucl. Data Sheets **112**, 2887 (2011).

[2]M. Mattes and J. Keinert, "Thermal neutron scattering data for the moderator materials H2O, D2O and ZrHx in ENDF-6 format and as ACE library for MCNP (X) codes. INDC (NDS)-0470," IAEA Technical Report, 2005.
[3]R. E. MacFarlane, "New thermal neutron scattering files for ENDF/B-VI release 2. LA–12639-MS," LANL Technical Report, 1994.
[4]K. Toukan and A. Rahman, Phys. Rev. B **31**, 2643 (1985).
[5]R. Bansil, T. Berger, K. Toukan, M. A. Ricci, and S. H. Chen, Chem. Phys. Lett. **132**, 165 (1986).
[6]G. Corongiu and E. Clementi, J. Chem. Phys. **98**, 4984 (1993).
[7]G. C. Lie and E. Clementi, Phys. Rev. A **33**, 2679 (1986).
[8]J. Marti, J. A. Padro, and E. Guardia, J. Chem. Phys. **105**, 639 (1996).
[9]Y. Lisichkin, L. Saharova, J. Marti, and A. Novikov, Mol. Simul. **31**, 1019 (2005).
[10]A. G. Novikov, A. A. Vankov, and L. S. Gosteva, J. Struct. Chem. **31**, 77 (1990).
[11]D. Van Der Spoel, E. Lindahl, B. Hess, G. Groenhof, A. E. Mark, and H. J. C. Berendsen, J. Comput. Chem. **26**, 1701 (2005).
[12]J. Martí, J. A. Padró, and E. Guàrdia, J. Mol. Liq. **62**, 17 (1994).
[13]M. A. González and J. L. F. Abascal, J. Chem. Phys. **135**, 224516 (2011).
[14]R. Mills, J. Phys. Chem. **77**, 685 (1973).
[15]J. Martí, E. Guàrdia, and J. A. Padró, J. Chem. Phys. **101**, 10883 (1994).
[16]S. E. Lappi, B. Smith, and S. Franzen, Spectrochim. Acta, Part A **60**, 2611 (2004).
[17]M. C. Bellissent-Funel, S. H. Chen, and J. M. Zanotti, Phys. Rev. E **51**, 4558 (1995).
[18]B. C. Haywood and D. I. Page, in *Proceedings of the Symposium on Neutron Thermalization and Reactor Spectra, Ann Arbor, MA* (IAEA, 1968), Vol. 1, p. 361.
[19]J. A. Padró and J. Martí, J. Chem. Phys. **118**, 452 (2003).
[20]P. Von Blanckenhagen, Ber. Bunsenges. Phys. Chem. **76**, 891 (1972).
[21]K. Larsson and U. Dahlborg, in *Proceedings of the Symposium on Inelastic Scattering of Neutrons*, Chalk River, Canada (IAEA, 1963), Vol. 1, p. 317.
[22]R. E. MacFarlane and D. W. Muir, "The NJOY nuclear data processing system, Version 99," LANL Technical Report, 1999.
[23]P. A. Egelstaff and P. Schofield, Nucl. Sci. Eng. **12**, 260 (1962).
[24]K. Sköld, Phys. Rev. Lett. **19**, 1023 (1967).
[25]A. K. Soper and C. J. Benmore, Phys. Rev. Lett. **101**, 065502 (2008).
[26]O. K. Harling, "Slow-neutron inelastic scattering and the dynamics of heavy water," BNWL Technical Report, 1968.
[27]F. Bischoff, W. A. Bryant, L. Esch, C. Lajeunesse, W. E. Moore, S. S. Pan, S. N. Purohit, and M. L. Yeater, "Low energy neutron inelastic scattering (LENIS) in linear accelerator project progress report RPI-328-27," RPI Technical Report, 1967.
[28]J. Teixeira, M. C. Bellissent-Funel, S. H. Chen, and A. J. Dianoux, Phys. Rev. A **31**, 1913 (1985).